The effect of an electrostatic field on the rupture of a thin viscous static film by van der Waals attractions

Hyo Kim[†]

Department of Chemical Engineering, The University of Seoul, 90 Jeonnong-dong, Dongdaemun-gu, Seoul 130-743, Korea
(*Received 7 February 2011 • accepted 1 April 2011*)

Abstract–This research examines rupture phenomena of a horizontal static thin viscous layer on a solid plate under an electrostatic field generating from a charged foil above the film. The dynamics of the electrified liquid film is formulated to derive a long-wave evolution equation of local film thickness. It determines two-dimensional nonlinear behavior of the film subject to surface tension, viscous, electrically induced forces, and van der Waals attractions. Linear stability analysis is used to obtain the maximum growth rate of a periodic disturbance and its corresponding wavenumber. To see the development of film rupture the strongly nonlinear partial differential equation is numerically solved for the unlimited or limited foil length as part of an initial-value problem with spatially periodic boundary conditions. The stronger electric forces make the thin layer more unstable and speed up its rupture.

Key words: Electrostatic Field, Rupture, Thin Viscous Static Film, van der Waals Attractions, Long-wave Evolution Equation

INTRODUCTION

The rupturing mechanism of thin liquid film is of significance in many engineering processes involving coalescence of droplets and bubbles in colloid and bicolloid systems, formation of dry spots on heated surfaces by an evaporating liquid film, and creation of rivulets on coating substrates, to name a few. In engineering applications the thin film has been highlighted in heat and mass transfer systems due to its high transfer surface compared to the volume of through-flow. When the thin layer encounters hydrodynamic instabilities, however, it easily leads to the loss of uniformity and breakdown into rupture.

Ruckenstein and Jain [1] studied spontaneous rupture of a thin liquid film on a solid surface. They modeled the liquid employing the Navier-Stokes equations with an additional body force. This body force was calculated from the potential energy per unit volume in the liquid caused by long-range molecular forces due to the London-van der Waals interactions with the surrounding molecules of the liquid and with those of the solid. Neglecting double layer forces, the body force is inversely proportional to the third power of the film thickness with Hamaker constant as its proportional constant. When the long-range van der Waals molecular forces are considered, a negative disjoining pressure which is characteristic of a film with a higher pressure than the bulk phase causes the thin layer to get thinning more and leads to spontaneous rupture [2]. Williams and Davis [3] applied a nonlinear stability theory on film rupture by investigating the stability of thin films to finite amplitude disturbances. They derived a partial differential equation describing the evolution of film thickness by including the van der Waals forces in the Navier-Stokes equations through the potential function proposed by Ruckenstein and Jain [1]. Burelbach et al. [4] dealt with the rupture phenomena of horizontal static liquid layers of either

evaporating or condensing to pay attention to the development of dryout on a planar solid. They discussed two-dimensional nonlinear stability of the layers subject to vapor recoil, thermocapillary, and rupture instabilities along with the effects of mass loss or gain.

Recently, another method of controlling the hydrodynamics of thin liquid film is through the applications of an electrostatic field such as to the designs of a thin liquid film radiator, microeletronics structure formation and pattern transfer, and bio-separation system. Kim et al. [5] first examined a liquid-metal film flowing down an inclined plane when a finite charged foil is placed at a fixed distance from the inclined plane. The normal electrostatic field exerts a tensile force on the liquid film and pulls it away from the plane. The solutions of film height evolution equation proposed by Kim et al. [5] were compared with the experimental observations by Griffing et al. [6] in 2006. Their two-dimensional height profiles were quite similar to the theoretical results obtained by Kim et al. [5]. Schäffer et al. [7] introduced a simple technique using an electric field to create and replicate lateral structures in polymer film. In addition, they [8] exploited the wave pattern caused by an electrohydrodynamic instability to get a non-equilibrium pattern formation in quasi-two-dimensional systems. Lin et al. [9] examined a systematic structure formation at the interface of liquid/liquid bilayers in an electric field. Blyth [10] investigated the effect of an electric field on a contaminated film flow down an inclined plane. He showed the major competition between the stabilizing influence of an insoluble surfactant and the destabilizing influence of an electric field on the film flow. Tseluiko et al. [11] studied two-dimensional nonlinear dynamics of electrified thin liquid films that are overlying or overhanging on a horizontal flat electrode. The electric field is generated from a second parallel electrode placed at a large vertical distance from the bottom plate. Through numerical experiments they present evidence for the global existence of positive periodic smooth solutions, indicating the film thins locally to zero after infinite time. For a rupturing process of a thin layer under an electric field, Tilley et al. [12] investigated the stability of a thin two-dimensional liquid sheet when a

---

uniform electric field is applied in a direction parallel to the initially flat bounding inviscid nonconducting liquid interfaces. In the same physical configuration as Tilley et al., Savettaseranee et al. [13] examined the rupture stability of thin viscous film sheets by calculating the competing effects of inertia, van der Waals attraction forces, surface tension, and electric fields. They found the electric field forces enhanced the stability of the flow and could remove rupture in the presence of a horizontal electric field.

However, when we have an electric field normal to a thin film, we anticipate its rupture could be accelerated because the normal electric field always acts as an instability. That is, the unstable layer has a local point to be ultra-thin (10-100 nm) and the van der Waals molecular forces will be present to cause the film to rupture and dewet the surface [4] [13]. Hence the present research will explain the rupture mechanism of a thin static film on a plane under a vertical electric field generated by a suspended charged foil.

FORMULATION

A thin horizontal liquid layer, e.g., water of thickness 10^{-6} cm, on a plane electrode is considered of an incompressible, Newtonian fluid having viscosity μ and density ρ. The liquid film with an undisturbed thickness d is assumed to be a perfect conductor and the air above the film to be a perfect dielectric. Within the air region there is a finite charged foil of length l having a constant electric field strength F at a distance H from the bottom plate. The electric field generated from the charged foil is assumed to act in the direction normal to the bottom wall. A two-dimensional coordinate system is chosen such that the x axis is parallel to the plane and the y axis is perpendicular to it, and let x=0 be at the center of the charged plate (Fig. 1). The liquid layer is sufficiently thin enough that gravity effects are negligible and van der Waals attractions are effective. It is interesting to model the rupture dynamics of static thin films affected by a vertical electrostatic field with the effects of attractive van der Waals forces.

The liquid region defined by $0 \le y \le h(t, x)$ and $-\infty \le x \le \infty$ is governed by the continuity and Navier-Stokes equations, and in the air phase above the liquid confined by $h(t, x) \le y \le H$ and $-\infty \le x \le \infty$ the electric field is satisfied by Laplace's equation for the electric volt-age V. There is no electric field within the liquid because it is assumed an electrically perfect conductor. As dimensional forms these equations are

$$\nabla \cdot u = 0, \tag{1}$$

$$\rho(u_t + u \cdot \nabla u) = -\nabla(p + \phi) + \mu \nabla^2 u, \tag{2}$$

$$\nabla^2 V = 0. \tag{3}$$

Here p denotes the pressure in the liquid, around 0.101 MPa in this system [4], and u is the liquid velocity vector with components (u, v) in the x- and y-directions, respectively. From Ruckenstein and Jain [1] the van der Waals forces are represented through the disjoining potential ϕ depending on the film thickness h, i.e.,

$$\phi = A' h^{-3}, \tag{4}$$

where A' is dimensional Hamaker constant, for water 10^{-13} erg. The density, viscosity, and velocity components in the air are neglected here because they are much smaller than in the liquid. The electric fields in the air are defined by

$$E = -\nabla V. \tag{5}$$

To solve Eq. (1)-(3) we need appropriate boundary conditions. On the solid plane wall, y=0, there is a no-slip boundary condition

$$u = 0. \tag{6}$$

Along the fluid interface, y=h(t, x), we have the jump mass balance

$$[(u - u^{(I)}) \cdot n]_{air}^{liquid} = 0, \tag{7}$$

where $u^{(I)}$ is the velocity of interface, and the jump shear-stress balance

$$[t \cdot T \cdot n]_{air}^{liquid} = 0, \tag{8}$$

and the jump normal-stress condition

$$[n \cdot T \cdot n]_{air}^{liquid} = \sigma \nabla \cdot n. \tag{9}$$

Here the subscripts means the partial derivatives, the jump notation $[*]_{air}^{liquid} = (*)^{liquid} - (*)^{air}$, t and n are unit tangent and outward unit normal vectors to the interface, respectively, and σ is the constant surface tension of the liquid. The stress tensor T is given by

$$T = -pI + \mu \nabla u + \varepsilon \left(EE - \frac{1}{2}|E|^2 I \right), \tag{10}$$

where I is the identity tensor, ε is the dielectric constant of the fluid, and the last term comes from Maxwell stresses at the interface [14]. The boundary conditions for the electrostatic field are given by

$$V = \begin{cases} FH, & \text{for } -l/2 \le x \le l/2 \\ 0, & \text{otherwise} \end{cases} \quad \text{at } y = H, \tag{11}$$

$$V = 0 \text{ at } y = h.$$

The product FH is a constant to scale the electric potential when F is the unit of electric field.

From now on, the governing equations and the boundary conditions are expressed in non-dimensional forms. By letting d and L be the units of length in the y and x directions, respectively, we introduce the slenderness parameter $\xi = d/L (\ll 1)$ to get a thin film limit, i.e., thin relative to the expected length scale of the disturbances in
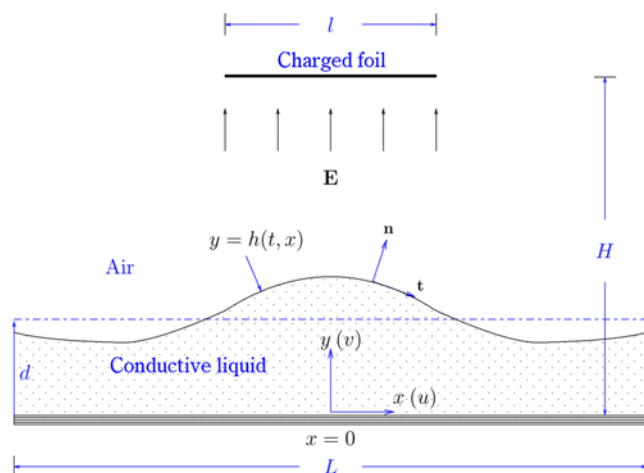

Fig. 1. The configuration of the thin film under a charged foil.

the horizontal. Choosing a characteristic velocity U_0 as ν/d based on a viscous scale, where ν is the kinematic viscosity of the liquid, U_0 is the unit of the x-direction velocity u, ξU_0 is the unit of the y-direction velocity v, L/U_0 is for the scale of time t, and ρU_0^2 is for the scales of pressure p and van der Waals potential ϕ. For convenience, all variables and parameters used hereafter are dimensionless, unless specified. The continuity equation becomes

$$u_x + v_y = 0, \tag{12}$$

while the x and y components of the momentum equation reduce to

$$\xi(u_t + uu_x + vu_y) = -\xi p_x - \xi \phi_x + (\xi^2 u_{xx} + u_{yy}) \tag{13}$$

and

$$\xi^2(v_t + uv_x + vv_y) = -p_y + \xi(\xi^2 v_{xx} + v_{yy}). \tag{14}$$

The dimensionless van der Waals potential ϕ can be written as

$$\phi = A\, h^{-3}, \tag{15}$$

where the dimensionless Hamaker constant A, for water $\sim 10^{-1}$, is related to A' by

$$A = \frac{A'}{6\pi d \rho \nu^2}. \tag{16}$$

Here it is assumed $A>0$, usually called the case of negative disjoining pressure [4]. It is worth noting that in case of water film the magnitude of the dimensionless hamaker constant, A, is slightly greater than the capillary number [4] (i.e., surface tension effect, defined below). From this, it is proven that the van der Waals effect plays a significant role in the film dynamics.

The boundary condition along the plate of y=0 is

$$u = 0, v = 0, \tag{17}$$

and on the interface of y=h(t, x) the boundary conditions of Eq. (7)-(9) become, respectively,

$$h_t + u\, h_x = v, \tag{18}$$

$$[1 - \xi^2 h_x^2](u_y + \xi^2 v_x) + 2\xi^2 h_x(v_y - u_x) = 0, \tag{19}$$

and

$$\frac{3\xi^2}{Ca} h_{xx}[1 + \xi^2 h_x^2]^{-\frac{3}{2}} = -p$$
$$+ 2\xi[\xi^2 h_x^2 u_x - h_x(u_y + \xi^2 v_x) + v_y][1 + \xi^2 h_x^2]^{-1} - 3K(E_n)^2. \tag{20}$$

Here the air pressure is neglected and E_n is the normal component of electric field to be determined later. From Eq. (20) the charged plate suspended above the thin film only influences the fluid motion via the inhomogeneous term in the normal stress equation. The dimensionless groups are a capillary number Ca and a dimensionless electric constant K. These are defined by

$$Ca = \frac{3\rho \nu^2}{d\sigma}, \tag{21}$$

and

$$K = \frac{\varepsilon_0 d^2 F^2}{24\pi \rho \nu^2}, \tag{22}$$

where ε_0 is the dielectric constant of the vacuum. The dimensionless forms of Laplace's equation for the electric field and the boundary conditions are reduced to

$$\xi^2 V_{xx} + V_{yy} = 0 \tag{23}$$

and

$$V = \begin{cases} 1, & \text{for } -l/2 \le x \le l/2 \\ 0, & \text{otherwise} \end{cases} \quad \text{at } y = H,$$
$$V = 0 \text{ at } y = h. \tag{24}$$

The dimensionless electric field is given by

$$E = -(\zeta V_x, HV_y), \tag{25}$$

with the normal and tangential components defined as $E_n = E \cdot n$ and $E_t = E \cdot t$, respectively. Here, ζ is the ratio of dimensional distance H to horizontal length L, which is assumed to be of order unity. Next, by using the long-wave theory taking $\xi \ll 1$, i.e., the film is very thin relative to the expected disturbances in x direction, a nonlinear evolution equation for h(t, x) will be derived for the linear stability and the dynamics of film rupture.

LONG-WAVE THEORY

To apply the asymptotic analysis to the governing system scaled to be consistent with lubrication theory, the dependent variables are expanded in powers of ξ:

$$u = u_0 + \xi u_1 + \cdots,$$
$$v = v_0 + \xi v_1 + \cdots,$$
$$p = \xi^{-1}(p_0 + \xi p_1 + \cdots),$$
$$\phi = \xi^{-1}(\phi_0 + \xi \phi_1 + \cdots). \tag{26}$$

Here to examine the spontaneous rupture of the film, p and ϕ are taken to be order of ξ^{-1}. To include the effects of surface tension and electrostatic field in the leading-order terms, $\xi K = \overline{K} = O(1)$ and $Ca/\xi^3 = \overline{Ca} = O(1)$ will be taken in the normal stress condition.

At leading order in ξ, the governing equations for the liquid phase are

$$\frac{\partial u_0}{\partial x} + \frac{\partial v_0}{\partial y} = 0, \tag{27}$$

$$\frac{\partial^2 u_0}{\partial y^2} - \frac{\partial p_0}{\partial x} - \frac{\partial \phi_0}{\partial x} = 0, \tag{28}$$

$$\frac{\partial p_0}{\partial y} = 0, \tag{29}$$

along with the boundary conditions

$$u_0 = v_0 = 0 \text{ at } y = 0, \tag{30}$$

and at y=h(t, x),

$$\frac{\partial h}{\partial t} + u_0 \frac{\partial h}{\partial x} = v_0, \tag{31}$$

$$\frac{\partial u_0}{\partial y} = 0, \tag{32}$$

and

$$\frac{3}{\overline{C}a}\frac{\partial^2 h}{\partial x^2} = -p_0 - 3\overline{K}(E_{0n})^2. \qquad (33)$$

The leading-order electric field can be obtained from the electrostatic potential at leading order in ξ, i.e., $E_{0n} = H(\partial V_0/\partial y)$, where V_0 is derived from the Eq. (23) with the boundary conditions in (24) by assuming $l \to \infty$ in order for the thin film analysis to be valid:

$$V_0 = (y-h)/(H-h), \text{ for } h(x, t) < y < H. \qquad (34)$$

Eqs. (27)-(34) yield a long-wave evolution equation governing the nonlinear stability of the thin film subject to rupture instability under a vertical electrostatic field. First, solve Eq. (29) with Eq. (32) and we get the pressure

$$p_0 = -3\left[\frac{1}{\overline{C}a}h_{xx} + \overline{K}(E_{0n})^2\right]. \qquad (35)$$

Insert the results from the differentiation of Eq. (15) and Eq. (35) with x into Eq. (28) and then solve it subject to conditions Eq. (30) and Eq. (32) to find the x-component of the liquid velocity,

$$u_0 = \left[\frac{1}{\overline{C}a}h_{xxx} + \overline{K}\frac{\partial}{\partial x}(E_{0n})^2 + A\frac{h_x}{h^4}\right]\left(3hy - \frac{3}{2}y^2\right), \qquad (36)$$

where $A = O(\xi^{-1})$ due to $\phi = O(\xi^{-1})$ as $\xi \to 0$. Eq. (16) is substituted into Eq. (27), which we then solve with the boundary condition Eq. (30), to find the y-component of the liquid velocity,

$$v_0 = -\frac{\partial}{\partial x}\left[\frac{1}{\overline{C}a}h_{xxx} + \overline{K}\frac{\partial}{\partial x}(E_{0n})^2 + A\frac{h_x}{h^4}\right]\left(\frac{3}{2}hy^2 - \frac{1}{2}y^3\right)$$
$$- \frac{3}{2}\left[\frac{1}{\overline{C}a}h_{xxx} + \overline{K}\frac{\partial}{\partial x}(E_{0n})^2 + A\frac{h_x}{h^4}\right]y^2 h_x. \qquad (37)$$

Finally, Eq. (36) and Eq. (37) at y=h are substituted into Eq. (31) to obtain the result

$$\frac{\partial h}{\partial t} + \frac{\partial}{\partial x}\left[\frac{1}{\overline{C}a}h_{xxx}h^3 + \overline{K}\frac{\partial}{\partial x}(E_{0n})^2 h^3 + A h_x h^{-1}\right] = 0, \qquad (38)$$

which represents a film evolution subject to surface tension, electrostatic force and van der Waals attraction. If there is no electrostatic field ($\overline{K}=0$), Eq. (38) reduces to that posed by Williams and Davis [3] subject to surface tension and van der Waals attractions. Employing the same rescaling procedure as taken by Burelbach et al. [4] which was initiated by Williams and Davis [3], we can remove the parameters $\overline{C}a$ and A, i.e., by letting

$$X = (\overline{C}aA)^{1/2}x, \quad T = (\overline{C}aA^2)t, \qquad (39)$$

and then obtain the final canonical form of the system:

$$\frac{\partial h}{\partial T} + \frac{\partial}{\partial X}\left[h_{XXX}h^3 + W\frac{\partial}{\partial X}(E_{0n})^2 h^3 + h_X h^{-1}\right] = 0, \qquad (40)$$

where $W = \overline{K}/A$. Before solving the single partial differential Eq. (40) with initial conditions, we need to employ linear stability theory to determine critical and maximum growth rates of disturbance and their corresponding wavelengths.

LINEAR STABILITY ANALYSIS

From the linear theory of Ruckenstein and Jain [1] as the layer

gets thinner than a critical value, infinitesimal disturbances begin to grow and the film attains zero thickness at some point. To perform the linear stability analysis we perturb the base state h=1 by a small parameter h′ which is directly related to the disturbance wavenumber α with the normal modes of the form,

$$h'(X, T) = \eta(T)e^{i\alpha X}. \qquad (41)$$

The resulting ordinary differential equation for the normal-mode amplitude η is

$$\frac{\dot{\eta}}{\eta} = \alpha^2\left[2\frac{WH^2}{(H-1)^3} + 1 - \alpha^2\right], \qquad (42)$$

where the dot means the derivative with T and $\dot{\eta}/\eta$ is the growth rate. From $\dot{\eta}/\eta = 0$, the cutoff wavenumber α_c is determined as

$$\alpha_c^2 = \left[2\frac{WH^2}{(H-1)^3} + 1\right], \qquad (43)$$

and any small disturbance grows for all $0 < \alpha < \alpha_c$. The wavenumber α_m for the maximum growth rate is given by $d(\dot{\eta}/\eta)/d\alpha = 0$ as

$$\alpha_m^2 = \left[\frac{WH^2}{(H-1)^3} + \frac{1}{2}\right]. \qquad (44)$$

Eq. (43) and Eq. (44) show that the applied electrostatic field makes the flow system more unstable to shorter wavelengths. In Fig. 2, the growth rate vs. α is plotted for W=0 and W=10 at H=20. When the electric force is ignored, Eq. (43) and Eq. (44) reduce to the same results obtained by Williams and Davis [3].

NUMERICAL SOLUTIONS

Eq. (40) is a strongly nonlinear partial differential equation which has to be numerically solved as part of an initial-value problem with spatially periodic solutions. Centered difference schemes in space are chosen on the periodic domain of $-\pi/\alpha \le X \le \pi/\alpha$, and the Crank-Nicolson method as an implicit scheme is applied for the time increment. The difference equations are solved by the Newton-Raphson iteration with the maximum tolerance of 10^{-10} where the generated matrices are manipulated by LU decomposition methods. Burelbach et al. [4] pointed in their calculation of rupture time T_R for evaporat-
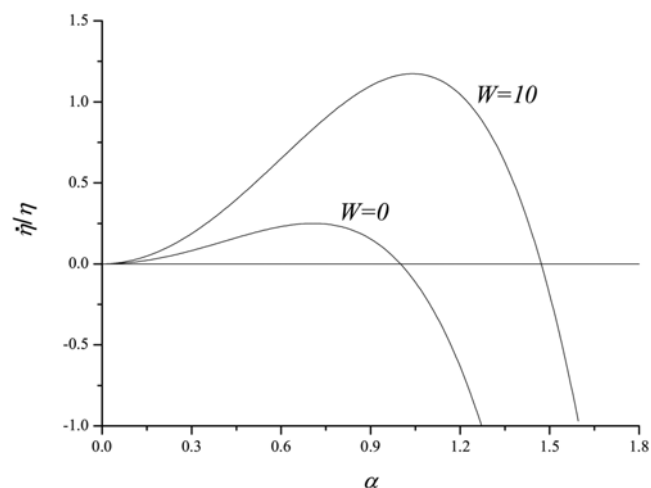

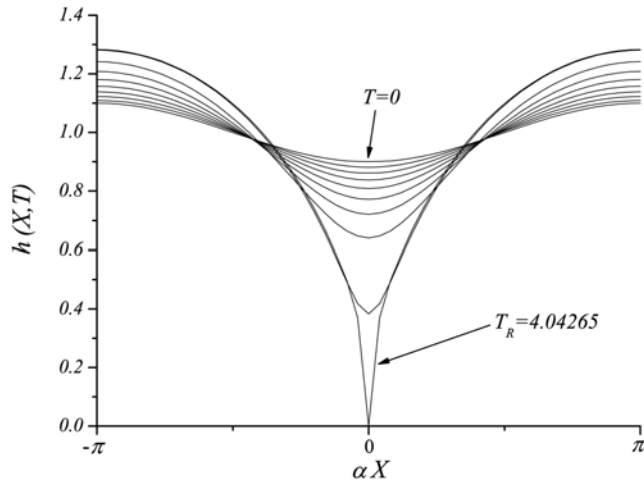Fig. 2. Growth rate vs. α for W=0 and W=10 at H=20.

Fig. 3. Film rupture evolution with $\alpha_m=1/\sqrt{2}$ at W=0.

Fig. 4. Film rupture evolution with $\alpha_m=1.04076$ with H=20 and W=10.

ing/condensing liquid films that spatial-mesh effects on the computing domain became unimportant when the number of spatial grid N within one wavelength λ was greater than 20 (mesh size $\Delta X < \lambda/20$). They showed the rupture time significantly decreased as the grid number approached to 20. Throughout all of the calculations they fixed N=40. Here N=50 is employed, that is, the disturbance wavelength is divided into N=50 equal elements to compute more accurate rupture time. To compare the rupture time with the result from Burelbach et al., we turn off the electric field and compute the rupture time with the same values as Burelbach et al. of $\alpha=\alpha_m=1/\sqrt{2}$, time step $\Delta T=10^{-3}$, and the initial condition:

$$h(0, X)=1-0.1\cos(\alpha X). \tag{45}$$

As shown in Fig. 3, the rupture time T_R is 4.04265 which is shorter than T_R=4.16394 obtained by Burelbach et al. [4], and it is confirmed greater grid numbers make it possible to get more accurate rupture time.

In the following subsections, film profiles and rupture times are computed for two charged-foil geometries, i.e., one is for $l\to\infty$ and the other is for a finite l. The case of infinite charged foil has been already considered in the linear stability analysis, so it can be checked how the applied electric strength makes the film unstable to the linear stability theory. Next, to take to more real situation it is desirable of considering a finite electrode affecting the rupture dynamics of a thin film.

1. For an Infinite Charged Foil ($l\to\infty$)

The infinite length of charged foil means it has the same dimension as the bottom electrode. In this case the film evolution Eq. (40) is solved with the initial condition Eq. (45), where $E_{0n}=H(\partial V_0/\partial y)$ is calculated by the potential of Eq. (34). The results of linear stability in Fig. 2 show the growing range of unstable wavenumber at W=10 is wider than that at no-electrified film (W=0). The maximizing wavenumber shifts from $\alpha_m=1/\sqrt{2}=0.70711$ at W=0 to $\alpha_m=1.04076$ at W=10, representing the thin layer becomes more unstable due to the electric field. The instability can be confirmed from the rupture-time calculation, that is, the rupture time at W=10 with $\alpha_m=1.04076$ is 1.32499 as shown in Fig. 4 which is much shorter than T_R=4.16394 at $\alpha_m=1/\sqrt{2}$ when W=0 (Fig. 3). In addition, at W=10 the minimum film thickness as function of time is plotted at two
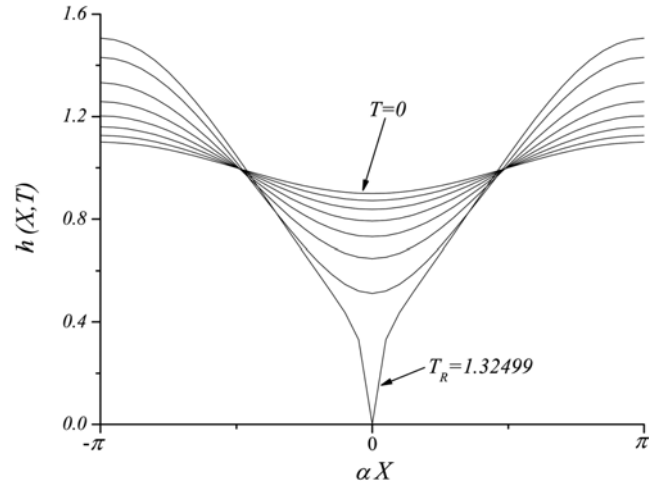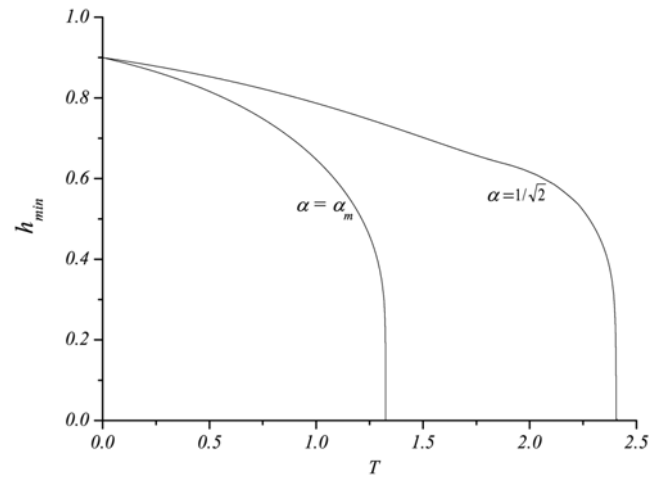

Fig. 5. Minimum film thickness as a function of time at α_m and $\alpha=1/\sqrt{2}$ when H=20 and W=10.

different wavenumbers, i.e., $\alpha=\alpha_m$ and $\alpha=1/\sqrt{2}$ which was the maximizing wavenumber when W=0, in Fig. 5. As time elapses the deepening speed of film thickness at the trough is more fast at α_m than at any other wavenumber until the liquid layer ruptures, which can be easily expected from the growth-rate graph (Fig. 2). In Fig. 6, to see how the applied electric field affects the rupture time we plot the rupture time T_R according to W. It is seen T_R decays exponentially as electric strength goes up.

2. For a Finite Charged Foil

To consider another geometric configuration of the charged foil, we let the length of foil be finite as shown in Fig. 1. Here when the thin layer is electrified by a suspended charged foil which is much smaller compared to the bottom electrode, the film succumbs to instability due to the pulling-over force induced in the direction normal to the initially flat interface. Before solving the nonlinear film evolution Eq. (40), first the distribution of the electric potential has to be obtained by solving the Laplace's equation of the electrostatic potential, i.e., $\nabla^2 V(X, y)=0$. To get the analytic solution of the Laplace's equation is very difficult because of the boundary condition, V=0
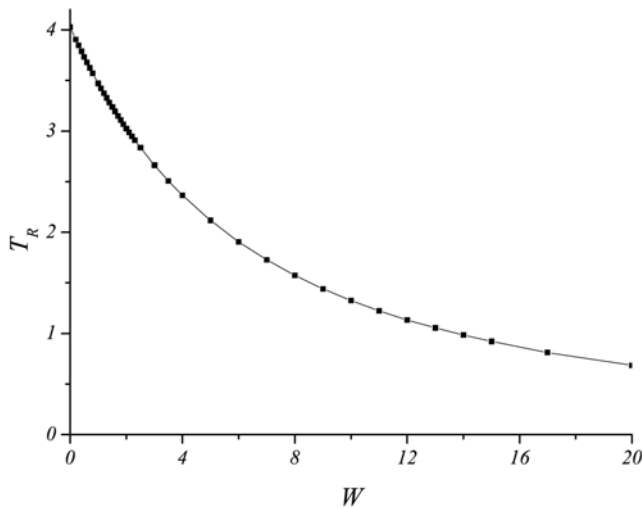
Fig. 6. Rupture time T_R vs. W at α_m and H=20.

Fig. 8. Rupture time T_R vs. W with α=0.2π, ξ=0.01, l=0.1 and H= 20.

at y=h where h is not constant. To overcome this difficulty we can assume H>>h so that the film is far away from the charged strip. And this kind of assumption is here very reasonable because the film is very thin as it ruptures. Hence the electric potential and the boundary conditions are given by

$$V_{xx}+V_{yy}=0 \tag{46}$$

and

$$V=\begin{cases} 1, & \text{for } -\bar{l}/2 \leq X \leq \bar{l}/2 \\ 0, & \text{otherwise} \end{cases} \quad \text{at } y=H, \tag{47}$$

$$V=0 \text{ at } y=0.$$

Here, $\bar{l}=(\overline{C}aA)^{1/2}l$.

The solution can be found in Morse and Feshbach [15] and the normal component of the electric field along the bottom electrode is given by Kim et al. [5] as

$$E_n=-1+\{1+e^{-(\pi/\xi H)[(\bar{l}/2)-X]}\}^{-1}+\{1+e^{-(\pi/\xi H)[(\bar{l}/2)+X]}\}^{-1}. \tag{48}$$

Eq. (48) can now be used in Eq. (40), and the resulting system is

solved numerically with the initial condition h(0, X)=1. This will describe the rupture dynamics of an electrified layer as soon as the suspended foil sets to be charged and then interacts with the initial undisturbed thin film. The only requirement for the validity of this computation is that H>>1. Fig. 7 shows the film profiles with α= 0.2π and ξ=0.01 at every T=1 until its breakage where the charged foil of l=1/10L locates at X=0 and y=H(=20). As we can expect the thin layer begins to swell up around the center of bottom plate where the charged foil exerts its force most strongly. When the film ruptures at T_R=8.75730, its final shape looks like a bud whose skirt builds up dryout points on the solid surface at the ends of bottom plate. And it has to be noted there are some quantitative differences in the behavior of film rupture when the electrostatic force exceeds a threshold value of W_{th}. The rupture appears to develop in a different way, that is, even with a slightly greater W than W_{th} the rupture occurs a little later rather than sooner. As W increases, the rupture time Decreases, as we can expect, but there shows up an inflection point of T_R at W=W_{th} as shown in Fig. 8 where T_R is plotted with
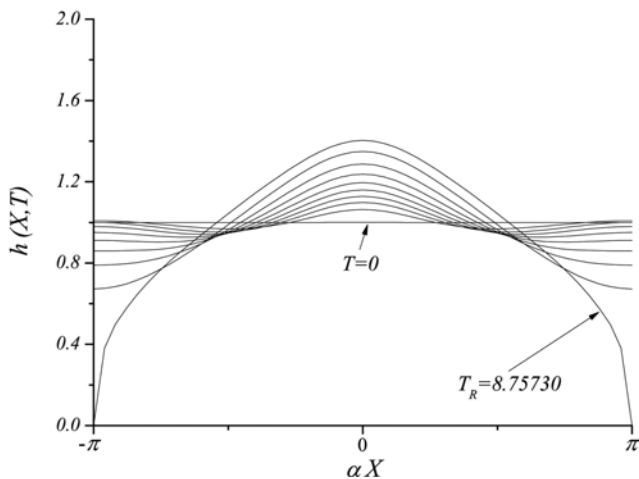

Fig. 7. Film rupture evolution with α=0.2π, ξ=0.01, l=0.1, H=20 and W=1.

Fig. 9. Film rupture evolution with α=0.2π, ξ=0.01, l=0.1, H=20 and W=1.7.

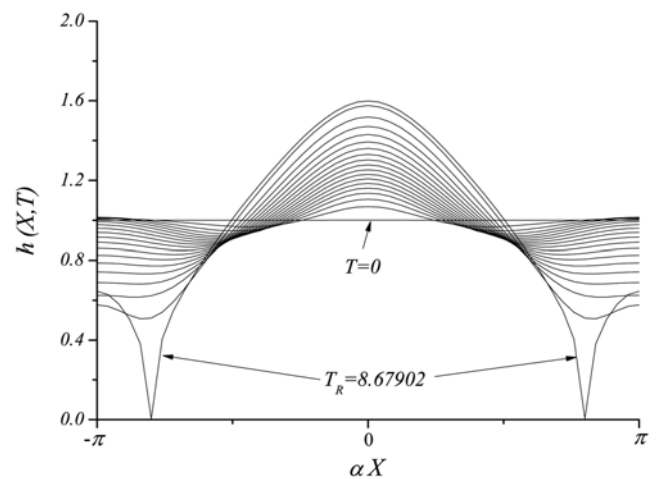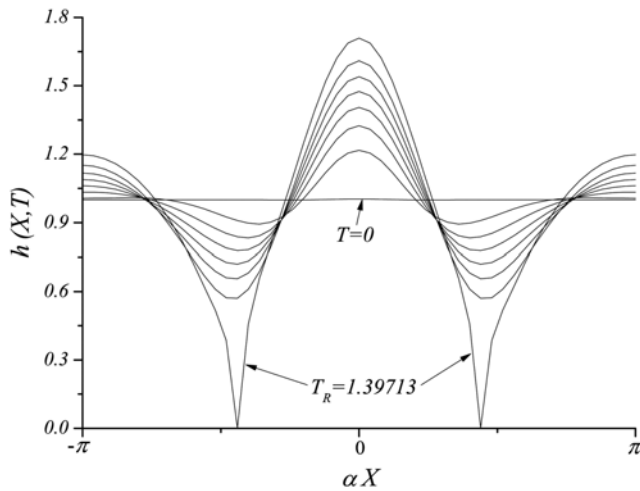**Fig. 10. Film rupture evolution with $\alpha=0.2\pi$, $\xi=0.01$, $l=0.1$, $H=20$ and $W=10$.**

W while keeping the other parameters as used in Fig. 7. Surprisingly, after W_{th} the rupture mechanism has a different mode such that the thin layer is divided into three parts as two breakup points locate inside of the layer. Fig. 9 describes well this kind of rupturing mode at $W=1.7(>W_{th}=1.6)$. Compared to Fig. 7 where all the liquid gathers to make a big lump when it shrinks at the end edges, however, in Fig. 9 the liquid is cut into three pieces as the rupture points take place within the film. It can be conjectured that breaking up the layer into three parts with two rupture points takes more time than there is no real layer breakage at $W<W_{th}$. Once the rupture points reside inside the region of the bottom electrode, as W increases the rupture time T_R is getting exponentially shorter (seen in Fig. 8) and the breakup points move closer to the center of the electrode. Fig. 10 shows the film rupture evolution with $\alpha=0.2\pi$, $\xi=0.01$, $l=0.1$, $H=20$ and $W=10$, where the stronger electric force compared to Fig. 9 makes the thin layer more unstable and speed up its rupture.

CONCLUSIONS

To answer the questions on the rupture dynamics of a horizontal static thin viscous layer on a solid plate under an electrostatic field from a charged foil above the film, a strongly nonlinear film evolution Eq. (40) is derived including the effects of surface tension, viscous, electric and van der Waals attraction forces. The long-range van der Waals molecular forces act as a negative disjoining pressure to cause a thin layer leading to spontaneous rupture, and at the same time when an electric field normal to a thin film is additionally applied, its rupture has been accelerated because the normal electric field always makes the film more susceptible to instabilities than when there is no electric force.

To show these instabilities quantitatively, both linear and nonlinear stabilities are analyzed according to Eq. (40), using numerical methods in the latter case. First, to examine the linear stability modes of the film rupture a small periodic disturbance in film height is applied to a flat layer and the cutoff wavenumber α_c and the maximum growth-rate wavenumber α_m are determined. Next, when it comes to nonlinear stability the strongly nonlinear partial differential equation is numerically solved for the unlimited or limited foil

length as part of an initial-value problem with spatially periodic boundary conditions. The Crank-Nicolson method is used as an implicit scheme for the time while the centered difference is employed in space with the spatial grid N=50. In case of an infinite foil length the nonlinear film profiles are well matched to the results anticipated from the linear stability analysis. When a finite charged foil is considered, there exists a threshold value of W_{th} describing a different rupturing mode, that is, as the electrostatic parameter W is increased and passes through W_{th}, a pair of rupture points appears out of the bottom solid plate. In less than W_{th} there is no real breakup of the layer and just a bud-like swollen liquid lump occupies whole region of the solid plate.

The applied electric forces make the thin layer more unstable and speed up its rupture. The non-dimensional parameter values are not necessarily physically realistic in this research.

NOMENCLATURE

A'	: dimensional Hamaker constant [erg]
A	: dimensionless Hamaker constant
Ca	: capillary number
$\overline{Ca}$	: Ca/ξ^3
d	: characteristic film thickness
E	: dimensionless electric field vector
E_n	: normal component of E
E_t	: tangential component of E
F	: unit of electric field
H	: dimensionless distance from plane to charged plate
I	: identity tensor
h	: dimensionless local film thickness
K	: dimensionless electric force constant
$\overline{K}$	: ξK
l	: dimensionless length of charged foil
$\overline{l}$	: $(\overline{Ca}A)^{1/2}l$
L	: characteristic length scale parallel to bottom plate
n	: unit normal vector
p	: dimensionless pressure
T	: $(\overline{Ca}A^2)t$
T	: stress tensor
t	: dimensionless time
t	: unit tangent vector
U_0	: characteristic velocity in x direction
u	: dimensionless velocity in x direction
V	: electrostatic potential
v	: dimensionless velocity in y direction
W	: $\overline{K}/A$
X	: $(\overline{Ca}A)^{1/2}x$
x	: dimensionless distance coordinate parallel to plane
y	: dimensionless distance coordinate perpendicular to plane

Greek Letters

α	: wavenumber

ε_0 : dielectric constant of vacuum
ε : dielectric constant of liquid
ζ : H/L
η : perturbation of h
λ : dimensionless wavelength
μ : dynamic viscosity of liquid
ν : kinematic viscosity of liquid
ξ : d/L
ρ : mass density of liquid
σ : surface tension of liquid
ϕ : dimensionless van der Waals potential

Superscripts
· : derivative with T
′ : small perturbation
(I) : interface of liquid and air

Subscripts
0 : leading order
c : cutoff value
m : maximum value
R : rupture
t : partial derivative with t
th : threshold value
X : partial derivative with X
x : partial derivative with x
y : partial derivative with y

REFERENCES

1. E. Ruckenstein and R. K. Jain, *Chem. Soc. Farady Trans.*, **70**, 132 (1974).
2. A. Scheludko, *Adv. Colloid Interface Sci.*, **1**, 391 (1967).
3. M. B. Williams and S. H. Davis, *J. Colloid Interface Sci.*, **90**, 220 (1982).
4. J. P. Burelbach, S. G. Bankoff and S. H. Davis, *J. Fluid Mech.*, **195**, 463 (1988).
5. H. Kim, S. G. Bankoff and M. J. Miksis, *Phys. Fluids A*, **4**, 2117 (1992).
6. E. M. Griffing, S. G. Bankoff, M. J. Miksis and R. A. Schluter, *ASME I: J. Fluids Eng.*, **128**, 276 (2006).
7. E. Schäffer, T. Thurn-Albrecht, T. P. Russell and U. Steiner, *Nature*, **403**, 874 (2000).
8. E. Schäffer, T. Thurn-Albrecht, T. P. Russell and U. Steiner, *Europhys. Lett.*, **53**, 518 (2001).
9. Z. Lin, T. Kerle, E. Schäffer, U. Steiner and T. P. Russell, *Macromolecules*, **35**, 3971 (2002).
10. M. G. Blyth, *J. Fluid Mech.*, **595**, 221 (2008).
11. D. Tseluiko and D. T. Papageorgiou, *SIAM J. Appl. Math.*, **67**, 1310 (2007).
12. B. S. Tilley, P. G. Petropoulos and D. T. Papageorgiou, *Phys. Fluids*, **13**, 3547 (2001).
13. K. Savettaseranee, D. T. Papageorgiou, P. G. Petropoulos and B. S. Tilley, *Phys. Fluids*, **15**, 641 (2003).
14. L. D. Landau, E. M. Lifshitz and L. P. Pitaevskii, *Electrodynamics of Continuous Media*, 2nd Ed., Pergamon, New York (1984).
15. P. M. Morse and H. Feshbach, *Methods of Theoretical Physics*, McGraw-Hill, New York (1953).